



Marine Polyphosphate: A Key Player in Geologic Phosphorus Sequestration

Julia Diaz, *et al.*
Science **320**, 652 (2008);
DOI: 10.1126/science.1151751

The following resources related to this article are available online at www.sciencemag.org (this information is current as of February 12, 2009):

Updated information and services, including high-resolution figures, can be found in the online version of this article at:

<http://www.sciencemag.org/cgi/content/full/320/5876/652>

Supporting Online Material can be found at:

<http://www.sciencemag.org/cgi/content/full/320/5876/652/DC1>

This article **cites 26 articles**, 5 of which can be accessed for free:

<http://www.sciencemag.org/cgi/content/full/320/5876/652#otherarticles>

This article has been **cited by** 3 article(s) on the ISI Web of Science.

This article appears in the following **subject collections**:

Oceanography

<http://www.sciencemag.org/cgi/collection/oceans>

Information about obtaining **reprints** of this article or about obtaining **permission to reproduce this article** in whole or in part can be found at:

<http://www.sciencemag.org/about/permissions.dtl>

2. T.-W. Chun *et al.*, *Proc. Natl. Acad. Sci. U.S.A.* **94**, 13193 (1997).
3. Q. E. Yang, *Med. Sci. Monit.* **10**, 155 (2004).
4. J. R. Siliciano *et al.*, *J. Infect. Dis.* **195**, 833 (2007).
5. J. Laurence, S. K. Sikder, S. Jhaveri, J. E. Salmon, *Biochem. Biophys. Res. Commun.* **166**, 349 (1990).
6. K. A. Roebuck, D. S. Gu, M. F. Kagnoff, *AIDS* **10**, 819 (1996).
7. S. Bocklandt, P. M. Blumberg, D. H. Hamer, *Antiviral Res.* **59**, 89 (2003).
8. A. Biancotto *et al.*, *J. Virol.* **78**, 10507 (2004).
9. J. Kulkosky *et al.*, *Blood* **98**, 3006 (2001).
10. Y. D. Korin, D. G. Brooks, S. Brown, A. Korotzer, J. A. Zack, *J. Virol.* **76**, 8118 (2002).
11. J. Kulkosky *et al.*, *AIDS Res. Hum. Retroviruses* **20**, 497 (2004).
12. R. J. Gulakowski, J. B. McMahon, R. W. Buckheit Jr., K. R. Gustafson, M. R. Boyd, *Antiviral Res.* **33**, 87 (1997).
13. M. Witvrouw *et al.*, *Antiviral Chem. Chemother.* **14**, 321 (2003).
14. J. Rullas *et al.*, *Antiviral Ther.* **9**, 545 (2004).
15. M. Hezareh *et al.*, *Antiviral Chem. Chemother.* **15**, 207 (2004).
16. S. A. Trushin *et al.*, *J. Virol.* **79**, 9821 (2005).
17. S. A. Williams *et al.*, *J. Biol. Chem.* **279**, 42008 (2004).
18. S. J. Brown *et al.*, paper presented at the 15th International AIDS Conference, Bangkok, Thailand, 11 to 16 June 2004 (abstract no. TuPeB4490), available at <http://gateway.nlm.nih.gov/MeetingAbstracts/102282312.html>.
19. F. J. Evans, R. G. Schmidt, *Acta Pharmacol. Toxicol. (Copenhagen)* **45**, 181 (1979).
20. A. R. Cashmore *et al.*, *Tetrahedron Lett.* **17**, 1737 (1976).
21. G. A. Miana, M. Bashir, F. J. Evans, *Planta Med.* **51**, 353 (1985).
22. P. A. Cox, *Pharm. Biol.* **39**, 33 (2001).
23. K. R. Gustafson *et al.*, *J. Med. Chem.* **35**, 1978 (1992).
24. H. Johnson, S. A. Banack, P. A. Cox, paper presented at the 48th Annual Meeting of Society for Economic Botany, Chicago, IL, 4 to 7 June 2007, available at www.econbot.org/_organization/_07_annual_meetings/meeting_abstracts/2007.php.
25. J. Hongpaisan, D. L. Alkon, *Proc. Natl. Acad. Sci. U.S.A.* **104**, 19571 (2007), and references therein.
26. H. Black, *Scientist* **18**, 59 (2004).
27. P. A. Wender *et al.*, *Curr. Drug Discov. Technol.* **1**, 1 (2004).
28. Z. Szallasi, L. Krsmanovic, P. M. Blumberg, *Cancer Res.* **53**, 2507 (1993).
29. D. A. Cairnes, S. S. Mirvish, L. Wallcave, D. L. Nagel, J. W. Smith, *Cancer Lett.* **14**, 85 (1981).
30. H. W. Thielmann, E. Hecker, *Liebigs Ann. Chem.* **728**, 158 (1969).
31. P. A. Wender *et al.*, *J. Am. Chem. Soc.* **111**, 8957 (1989).
32. P. A. Wender, F. E. McDonald, *J. Am. Chem. Soc.* **112**, 4956 (1990).
33. P. A. Wender, K. D. Rice, M. E. Schnute, *J. Am. Chem. Soc.* **119**, 7897 (1997).
34. M. Gschwendt, E. Hecker, *Tetrahedron Lett.* **11**, 567 (1970).
35. M. Hirota *et al.*, *Cancer Res.* **48**, 5800 (1988).
36. W. Haas, H. Sterk, M. Mittelbach, *J. Nat. Prod.* **65**, 1434 (2002).
37. D. Fairless, *Nature* **449**, 652 (2007).
38. V. W. Bowry, K. U. Ingold, *J. Am. Chem. Soc.* **114**, 4992 (1992).
39. H. Bartsch, E. Hecker, *Z. Naturforsch. Teil B* **24**, 91 (1969).
40. Materials and methods are detailed in supporting material available on Science Online.
41. P. S. Engel, L. Shen, *Can. J. Chem.* **52**, 4040 (1974).
42. J. P. Freeman, *J. Org. Chem.* **29**, 1379 (1964).
43. For an example of demonstrated technology for large-scale organic photolysis, see (46).
44. J. E. H. Buston, T. D. W. Claridge, M. G. Moloney, *J. Chem. Soc. Perkin Trans. 2* **1995**, 639 (1995).
45. S.-S. Tseng, B. L. Van Duuren, J. J. Solomon, *J. Org. Chem.* **42**, 3645 (1977).
46. B. D. A. Hook *et al.*, *J. Org. Chem.* **70**, 7558 (2005).
47. We thank T. Benvegna and T. Storz-Eckerlin (Stanford University) for exploratory studies on this project. This work was supported by grants from NIH to P.A.W. (CA31841 and CA31845).

Supporting Online Material

www.sciencemag.org/cgi/content/full/320/5876/649/DC1
Materials and Methods

28 December 2007; accepted 12 March 2008
10.1126/science.1154690

Marine Polyphosphate: A Key Player in Geologic Phosphorus Sequestration

Julia Diaz,¹ Ellery Ingall,^{1*} Claudia Benitez-Nelson,² David Paterson,^{3†} Martin D. de Jonge,^{3†} Ian McNulty,³ Jay A. Brandes⁴

The in situ or authigenic formation of calcium phosphate minerals in marine sediments is a major sink for the vital nutrient phosphorus. However, because typical sediment chemistry is not kinetically conducive to the precipitation of these minerals, the mechanism behind their formation has remained a fundamental mystery. Here, we present evidence from high-sensitivity x-ray and electro dialysis techniques to describe a mechanism by which abundant diatom-derived polyphosphates play a critical role in the formation of calcium phosphate minerals in marine sediments. This mechanism can explain the puzzlingly dispersed distribution of calcium phosphate minerals observed in marine sediments worldwide.

Phosphorus is a vital macronutrient that profoundly influences global oceanic primary production on both modern and geologic time scales (1, 2). Over the past several decades, the residence time of phosphorus in the ocean has been repeatedly revised downwards as previously unidentified sedimentary sinks have been discovered (1, 3). Among these sinks are ubiquitous fine-grained authigenic apatite minerals (4), whose origin is enigmatic (5). Given the strong influence of this mineral sink on the global cycling of phosphorus and its potential impact on long-term nu-

trient availability and biological production, an understanding of the underlying mechanisms that lead to the formation and burial of apatite in modern and ancient sediments is critically important. Here, we show that polyphosphate is a key component in the formation of apatite in marine sediments.

Polyphosphate is a relatively understudied component of the marine phosphorus cycle. A linear polymer of orthophosphate units linked by phosphoanhydride bonds (fig. S1), polyphosphate is present in cells as dense, calcium-associated cytoplasmic inclusions (6). Under phosphate-enriched conditions, cultured marine algae synthesize polyphosphate as a luxury nutrient reserve (7–12). The biological synthesis of substantial amounts of polyphosphate in natural marine systems, in contrast, has been hypothesized to be inconsequential (12), as phosphorus is present at biologically limiting concentrations in much of the global ocean (1, 3). Correspondingly, investigations into the composition of marine biogenic phosphorus compounds have typically focused

on organic forms (1, 13). The lack of commonly used analytical techniques that cleanly evaluate polyphosphate within samples has further resulted in a paucity of research on the importance of this phase. With the recent development of high-resolution x-ray spectromicroscopy methods, various particulate organic, mineral, and polymeric phosphorus-containing phases like polyphosphate can now be identified and mapped at submicrometer scales. In addition, a new combined electro dialysis/reverse osmosis technique allows for a more comprehensive examination of phosphorus composition in the dissolved phase. We have developed insights into the origin and transformation of marine polyphosphate through the application of these high-resolution x-ray (14) and high-recovery electro dialysis (15, 16) techniques.

We collected organisms, sediments, and dissolved and particulate matter during April and July 2007 from Effingham Inlet, a Pacific fjord located on Vancouver Island, British Columbia (fig. S2) (16). During the spring bloom of April 2007, intracellular polyphosphate inclusions were observed in individual diatoms, including the globally ubiquitous and abundant *Skeletonema* spp. (fig. S3). On the basis of bulk ³¹P- nuclear magnetic resonance (NMR) characterization of the spring bloom plankton community (16), inorganic polyphosphate represented a substantial 7% of total phosphorus in surface water biomass. Surface water dissolved phosphate concentrations were 0.5 μM, which reflects a level of phosphorus availability typical of coastal marine systems. Nutrient ratios were also consistent with phosphorus limitation in our field site (nitrogen:phosphorus = ~40). By comparison, in laboratory cultures with enriched, ~μM phosphate concentrations, *Skeletonema* spp. and *Thalassiosira* spp. can accumulate polyphosphate to correspondingly

¹School of Earth and Atmospheric Sciences, Georgia Institute of Technology, Atlanta, GA 30332-0340, USA. ²Marine Science Program and Department of Geological Sciences, University of South Carolina, Columbia, SC 29208, USA. ³Advanced Photon Source, Argonne National Laboratory, 9700 South Cass Avenue, Argonne, IL 60439, USA. ⁴Skidaway Institute of Oceanography, 10 Ocean Science Circle, Savannah, GA 31411, USA.

*To whom correspondence should be addressed. E-mail: ingall@eas.gatech.edu

†Present address: Australian Synchrotron, 800 Blackburn Road, Clayton, Victoria 3168, Australia.

high levels of 30% and 19 to 43% of total cellular phosphorus, respectively (10, 12). The population of diatom-dominated plankton in Effingham Inlet exhibited near-Redfield elemental stoichiometry, with a molar C:N:P composition of 188:16:1. The presence of substantial polyphosphate in these organisms thus appears not to alter their elemental content relative to the classic composition of marine phytoplankton. This finding suggests that inorganic polyphosphate has conventionally been quantified as a component of organic biomass and is not inconsistent with Redfield stoichiometry.

Polyphosphate can exist within a range of sizes and molecular weights inside cells, depending on the length of the polyphosphate polymer. Destruction of polyphosphate-containing diatoms by zooplankton grazing, viral infection, and senescence may liberate the intracellular contents

of these cells, including variably sized polyphosphate inclusions. Consistent with these processes, we observed a substantial amount of polyphosphate in the <0.45- μm fraction of dissolved matter (16). In subsurface seawater samples processed by the high-recovery electro dialysis/reverse osmosis technique (15), polyphosphate accounted for ~11% of the total dissolved phosphorus pool. Previous dissolved matter characterizations do not report polyphosphate (17–19), probably because of the lower-recovery methods used in these studies. By adding the critical step of deionizing seawater samples before concentrating dissolved molecules, the combined electro dialysis/reverse osmosis technique can isolate up to 90% of marine dissolved matter, the highest recovery yet possible (15).

In addition to dissolved matter, polyphosphate was also present in sinking particles, representing 7% of total phosphorus in sinking material (16).

Table 1. Key chemical parameters of major phosphorus pools. Polyphosphate content for each pool was measured by ^{31}P -NMR. Total phosphorus (% total P) and weight percent (wt %) biogenic silica content were determined by standard chemical techniques (16). Where available, error estimates represent measurement reproducibility on the basis of replicate analyses. Analytical errors associated with the polyphosphate measurement are $\pm 10\%$ of the reported value. For example, a polyphosphate measurement of 7% would have an associated error of $\pm 0.7\%$. Replicate total phosphorus measurements agreed to within <5%.

Phosphorus pool	Polyphosphate (% total P)	Total P ($\mu\text{mol g}^{-1}$)	Biogenic silica (wt %)
Plankton	7	123.0 ± 1.7	40.4 ± 1.4
Dissolved matter	11	1.72*	—
Sinking particles	7	59.76 ± 0.42	43.7 ± 2.3
Surface sediment	8†	44.71	12.08 ± 0.65

*Units are μM . †Data are from (24).

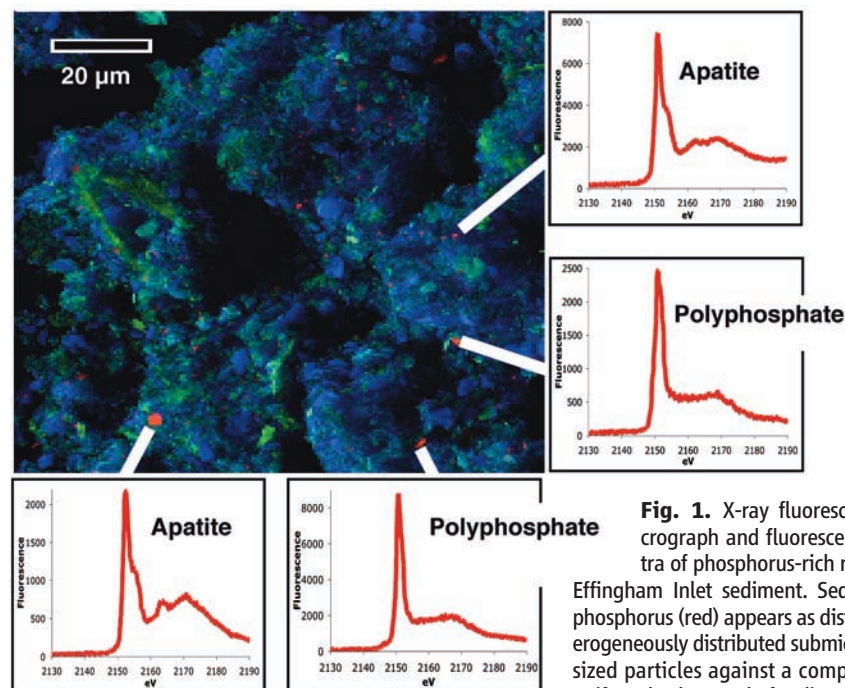


Fig. 1. X-ray fluorescence micrograph and fluorescence spectra of phosphorus-rich regions in Effingham Inlet sediment. Sedimentary phosphorus (red) appears as distinct, heterogeneously distributed submicrometer-sized particles against a comparatively uniform background of sedimentary aluminum (blue) and magnesium (green). On the basis of high-resolution x-ray spectroscopic characterization, about half of the 147 phosphorus-rich regions examined in our samples were found to be polyphosphate, whereas the other half were classified as apatite, a common calcium phosphate mineral.

Individual diatoms containing intracellular polyphosphates were observed throughout the water column, which suggests that sinking polyphosphate reaches the sediment protectively encased within intact cells. In fact, diatoms have been shown to play major roles in the mineral-ballasted transport of material to depth (20, 21). Table 1 summarizes our results on the polyphosphate, total phosphorus, and biogenic silica composition of major phosphorus pools investigated in this study. Mass balance estimates based on these data demonstrate that plankton-derived polyphosphate can account for the entire polyphosphate content of sinking particles. To make this calculation, the concentration of polyphosphate in plankton and sinking material can be expressed relative to biogenic silica content, which is roughly conserved between these two pools. Using the total phosphorus concentrations of plankton and sinking particles, the silica-normalized polyphosphate content of sinking material is ~45% of that in organisms. This estimate, although based on a single particle flux measurement, shows that plankton are a plausible and sufficient source for the polyphosphate found in sinking material.

Bacterial decomposition of the organic diatom frustule matrix results in rapid dissolution of the mineral shell (22) and the consequent release of polyphosphate and other cellular contents to the sediment environment. This scenario is consistent with the relatively low biogenic silica content of Effingham Inlet surface sediments (Table 1) and with microscopy results showing damaged and vacant diatom frustules in sediments. In addition, high-resolution x-ray spectromicroscopy methods (14, 23) revealed an abundance of free 0.5- to 3- μm polyphosphate granules in surface sediments (16). This size range is similar to that observed within diatoms, again suggesting a diatom source.

X-ray fluorescence data indicated that among the hundreds of phosphorus-rich particles identified in our sediment samples, ~50% were polyphosphate, with the remaining fraction composed of apatite, a common calcium phosphate mineral (Fig. 1). Previous ^{31}P -NMR analysis of Effingham Inlet surface sediments has shown that polyphosphate accounts for 8% of the total phosphorus in surface sediment samples (24). In other studies, polyphosphate has eluded detection by bulk techniques such as ^{31}P -NMR because such methods are relatively insensitive to the presence of less prevalent phases. Because synchrotron-based x-ray spectromicroscopy is unique in its capacity to simultaneously image and chemically characterize minimally prepared particulate samples at submicrometer resolution, this highly sensitive method is key to the direct identification of less prevalent phases in a wide variety of environments (14).

Our findings demonstrate that marine polyphosphate accounts for 7 to 11% of the phosphorus in dissolved and particulate pools (Table 1). This level of abundance is comparable to that of

more commonly identified organic phosphorus forms. For example, phosphonates typically represent ~3% of total phosphorus in fresh organic matter (25). The relative polyphosphate contents of plankton, sinking particulates, and sediments are nearly identical in our samples (Table 1). The consistency of the polyphosphate signal throughout the water column and surface sediment suggests that extracellular polyphosphate may not be readily bioavailable. Rapid enzymatic hydrolysis of polyphosphate by benthic microbes has been observed to occur, but only intracellularly (26). Because the phosphoanhydride bonds linking orthophosphate units of polyphosphate are relatively stable in the absence of hydrolytic enzymes (6), free sedimentary polyphosphate may be an efficient storage form of phosphorus over long periods. Consistent with this idea, x-ray analysis revealed the presence of extracellular polyphosphate in Effingham Inlet sediments up to 60 years old, which suggests that a portion of the free sedimentary polyphosphate pool is not remobilized over decadal time scales.

Though a portion of the sedimentary polyphosphate pool may be relatively stable, mass balance calculations reveal that some polyphosphate is removed from surface sediments over relatively short time scales. Using the bulk sediment trap flux from our field site ($136 \text{ g m}^{-2} \text{ year}^{-1}$), we estimated the sedimentary flux of polyphosphate to be $48 \mu\text{g P m}^{-2} \text{ day}^{-1}$ (16). The accumulation rate of polyphosphate in recent (<3-year-old) sediments from Effingham Inlet is 86% of this flux, based on the polyphosphate and total phosphorus content of surface sediments (Table 1). This disparity reflects a 14% loss of polyphosphate in surface sediments, a loss that may increase as sediments age.

The loss of sedimentary polyphosphate in sediments does not necessarily indicate that phosphorus is remobilized from polyphosphate particles. Rather, as evidence from x-ray spectromicroscopy reveals, the relative stability of free sedimentary polyphosphate permits diagenetic transformations that result in the long-term sequestration of phosphorus. In addition to demonstrating that polyphosphate and apatite are prevalent in sediments from Effingham Inlet, results from x-ray spectromicroscopy also showed an abundance of fine, dispersed particles that exhibit spectral features transitional between pure polyphosphate and apatite (Fig. 2). Polyphosphate thus appears to nucleate authigenic apatite growth, thereby converting surface water derived polyphosphate to stable phosphorus containing mineral phases that reside in sediments over geologic time scales.

Authigenic apatite formation in marine sediments has been recognized in numerous studies as an important phosphorus sink (4). However, the processes leading to the precipitation and growth of these authigenic apatites are not well understood. Massive apatitic phosphorite deposits that account for as much as 25% of total phosphorus in the sediments underlying major

coastal upwelling zones may be related to the activity of polyphosphate-accumulating sulfur bacteria (26). Enzymatic hydrolysis of intracellular polyphosphate by these bacteria releases considerable amounts of dissolved phosphate to sediment pore waters. As a result, pore waters achieve the high degree of supersaturation required to overcome the kinetic nucleation barrier to apatite precipitation, and substantial apatite formation consequently occurs (26).

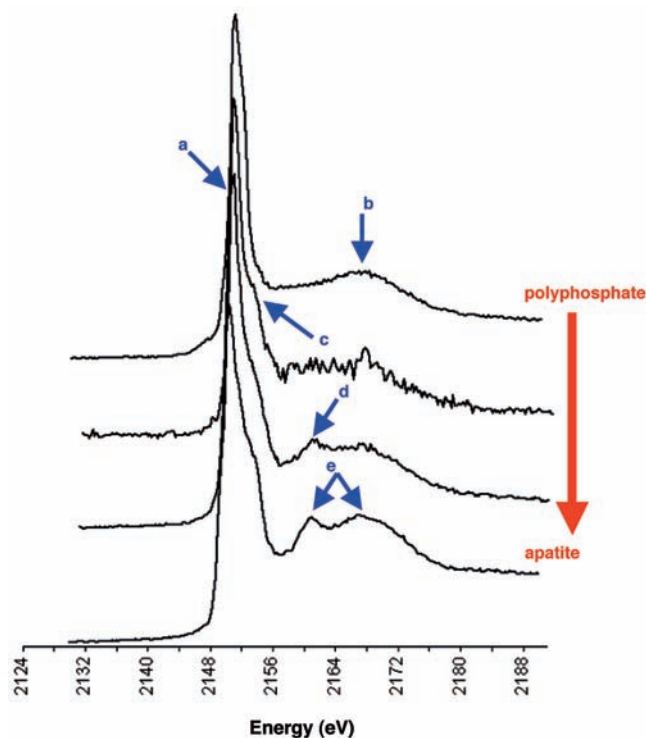
In contrast to the massive apatite-rich phosphorite formations characteristic of coastal upwelling zones, most marine sediments worldwide possess dispersed, fine-grained authigenic apatites that make up a comparatively small 9 to 13% of total sedimentary phosphorus (4). The relatively modest accumulation of authigenic apatite that is typical of sediments in nonupwelling zones nevertheless represents a substantial phosphorus sink because of the much larger areal extent of these environments (4). Authigenic apatite formation in these nonupwelling areas may not involve an episodic mechanism to produce high concentrations of dissolved phosphate, however. Rather, our results show that dispersed grains of sedimentary polyphosphate may nucleate apatite growth directly and nonepisodically, reducing or removing the nucleation barrier by acting as a mineral template. As noted previously, calcium is associated with polyphosphate in cells (6). The presence of highly concentrated sedimentary phosphorus regions with this calcium association may result in eventual apatite formation without

extensive interaction with the free sedimentary phosphate pool. We observed the transition from polyphosphate to apatite within surficial sediments <3 years of age, suggesting that apatite formation from a polyphosphate template may occur over relatively short time scales.

The transport of polyphosphate from its planktonic origin in surface waters to underlying sediments, followed by the subsequent diagenetic transformation into stable calcium phosphate minerals, provides a “biological pump” mechanism for the geologic sequestration of water column-derived marine phosphorus (fig. S4). The polyphosphate-accumulating diatoms observed in this study are common in the global ocean, including vast regions of coastal and polar seas that exhibit similar phosphate availability to our sampling site (27). Therefore, the sequestration of phosphorus through mechanisms involving diatom-derived polyphosphate is likely to be quantitatively substantial on a global scale.

Another documented source of polyphosphate in natural marine systems involves synthesis by benthic sulfur-oxidizing bacteria (26), yet these organisms thrive in specialized environments and are not as globally prevalent as diatoms. Polyphosphate has been identified in *Trichodesmium* spp. and other common marine cyanobacteria (7–9), suggesting that these organisms may be an important source of polyphosphate in the tropical and subtropical oceans where they are abundant. An abiological origin for polyphosphate is unlikely in most marine environments because abi-

Fig. 2. Diagenetic transformation of polyphosphate to apatite. An overlay of phosphorus x-ray fluorescence spectra collected from micrometer-sized phosphorus-rich regions in Effingham Inlet sediment illustrates the diagenetic transition from polyphosphate (**top**) to apatite (**bottom**). The primary phosphorus fluorescence peak occurs at 2150 eV (a). Spectral features above the primary peak reflect the local bonding environment of phosphorus. Polyphosphate, a simple linear polymer associated with calcium in cells, is characterized by a single peak 18 eV above the primary peak (b). In the diagenetic transition from polyphosphate to apatite, the association between phosphorus and calcium becomes more crystalline, which may account for the appearance of a primary peak “shoulder” (c). As the crystalline mineral matrix develops further, a peak 11 eV above of the primary peak appears (d), and secondary peaks become more defined (e). The spectra presented in this figure were collected from a single Effingham Inlet sediment sample <3 years of age. Thus, the relative ages of the particles that yielded these spectra are not known.



otic polyphosphate synthesis can only occur at the elevated temperatures characteristic of such extreme environments as hydrothermal vent systems (6). There is no evidence that the transformation of polyphosphate to apatite in marine sediments is dependent on the specific source of polyphosphate, however.

Enhanced phosphorus sequestration in marine sediments resulting from the conversion of diatom-derived polyphosphates to apatite may be manifested in the geologic record. The mid-Mesozoic rise of marine diatoms (28) coincides with a trend toward lower organic carbon to total phosphorus ratios in marine sediments (29). Because oceanic phosphorus influences atmospheric carbon dioxide levels over geologic time through regulation of marine primary productivity (2), geologic fluctuations in phosphorus burial efficiency brought on by changes in diatom abundance may have also exerted substantial paleoclimatic influences.

References and Notes

1. C. R. Benitez-Nelson, *Earth Sci. Rev.* **51**, 109 (2000).
2. P. Van Cappellen, E. D. Ingall, *Science* **271**, 493 (1996).
3. A. Paytan, K. McLaughlin, *Chem. Rev.* **107**, 563 (2007).
4. K. C. Ruttenberg, R. A. Berner, *Geochim. Cosmochim. Acta* **57**, 991 (1993).

5. P. Van Cappellen, R. A. Berner, *Geochim. Cosmochim. Acta* **55**, 1219 (1991).
6. M. R. W. Brown, A. Kornberg, *Proc. Natl. Acad. Sci. U.S.A.* **101**, 16085 (2004).
7. P. Mateo, I. Douterelo, E. Berrendero, E. Perona, *J. Phycol.* **42**, 61 (2006).
8. K. M. Romans, E. J. Carpenter, *J. Phycol.* **30**, 935 (1994).
9. B. A. Lawrence *et al.*, *Microbiology* **169**, 195 (1998).
10. L. Solorzano, J. D. H. Strickland, *Limnol. Oceanogr.* **13**, 515 (1968).
11. K. Miyata, A. Hattori, A. Ohtsuki, *Mar. Biol.* **93**, 291 (1986).
12. M. J. Perry, *Limnol. Oceanogr.* **21**, 88 (1976).
13. D. M. Karl, K. M. Björkman, in *Biogeochemistry of Marine Dissolved Organic Matter*, D. A. Hansell, C. A. Carlson, Eds. (Academic Press, New York, 2002), chap. 6.
14. J. A. Brandes, E. Ingall, D. Paterson, *Mar. Chem.* **103**, 250 (2007).
15. T. A. Vetter, E. M. Perdue, E. Ingall, J.-F. Koprivnjak, P. H. Pfomrom, *Sep. Purif. Technol.* **56**, 383 (2007).
16. Materials and methods are available as supporting material on Science Online.
17. L. L. Clark, E. D. Ingall, R. Benner, *Am. J. Sci.* **299**, 724 (1999).
18. L. C. Kolowitz, E. D. Ingall, R. Benner, *Limnol. Oceanogr.* **46**, 309 (2001).
19. P. Sannigrahi, E. D. Ingall, R. Benner, *Geochim. Cosmochim. Acta* **70**, 5868 (2006).
20. K. O. Buesseler *et al.*, *Science* **316**, 567 (2007).
21. R. A. Armstrong, C. Lee, J. I. Hedges, S. Honjo, S. G. Wakeham, *Deep-Sea Res. II* **49**, 219 (2001).
22. K. Biddle, F. Azam, *Nature* **397**, 508 (1999).
23. X-ray fluorescence spectra and phosphorus elemental maps were collected at beamline 2-ID-B, Advanced Photon Source, Argonne National Laboratory.
24. P. Sannigrahi, E. Ingall, *Geochem. Trans.* **6**, 52 (2005).
25. L. L. Clark, E. D. Ingall, R. Benner, *Nature* **393**, 426 (1998).
26. H. N. Schulz, H. D. Schulz, *Science* **307**, 416 (2005).
27. F. Louanchi *et al.*, *Deep-Sea Res. I* **48**, 1581 (2001).
28. M. E. Katz, Z. V. Finkel, D. Grzebyk, A. H. Knoll, P. G. Falkowski, *Annu. Rev. Ecol. Syst.* **35**, 523 (2004).
29. T. J. Algeo, E. Ingall, *Palaeogeogr. Palaeoclimatol. Palaeoecol.* **256**, 130 (2007).
30. This material is based on work supported by NSF under grant 0526178. Use of the Advanced Photon Source is supported by the U.S. Department of Energy, Office of Basic Energy Sciences (DE-AC02-06CH11357). We thank the crew of the R/V Barnes; R. Keil and J. Nuwer for assistance with field sampling; S. Herron and G. Lyons for help during field sampling and sample analysis; R. Styles and C. Jackson for assistance with sample analysis; G. Patterson and J. Platenius of the Clayoquot Field Station in Tofino, British Columbia, for providing lab space and a welcoming base for our field studies; P. Sobocky and members of her lab at Georgia Tech for the use of the epifluorescence microscope, and J. Leisen and L. Gelbaum for NMR assistance. The authors declare no competing financial interests.

Supporting Online Material

www.sciencemag.org/cgi/content/full/320/5876/652/DC1

Materials and Methods

SOM Text

Figs. S1 to S9

References and Notes

15 October 2007; accepted 24 March 2008

10.1126/science.1151751

Expanding Oxygen-Minimum Zones in the Tropical Oceans

Lothar Stramma,^{1*} Gregory C. Johnson,² Janet Sprintall,³ Volker Mohrholz⁴

Oxygen-poor waters occupy large volumes of the intermediate-depth eastern tropical oceans. Oxygen-poor conditions have far-reaching impacts on ecosystems because important mobile macroorganisms avoid or cannot survive in hypoxic zones. Climate models predict declines in oceanic dissolved oxygen produced by global warming. We constructed 50-year time series of dissolved-oxygen concentration for select tropical oceanic regions by augmenting a historical database with recent measurements. These time series reveal vertical expansion of the intermediate-depth low-oxygen zones in the eastern tropical Atlantic and the equatorial Pacific during the past 50 years. The oxygen decrease in the 300- to 700-m layer is 0.09 to 0.34 micromoles per kilogram per year. Reduced oxygen levels may have dramatic consequences for ecosystems and coastal economies.

Oceanic dissolved-oxygen concentrations affect marine biogeochemical processes and have major impacts on the global carbon and nitrogen cycles (1). These concentrations are very sensitive to changes in air-sea fluxes and interior ocean advection, hence dissolved oxygen is an important parameter for understanding the ocean's role in climate (2). Impor-

tant mobile macroorganisms are stressed or die under hypoxic conditions; that is, when oxygen concentrations drop below ~60 to 120 $\mu\text{mol kg}^{-1}$ (3). Hypoxia occurs at different oxygen concentrations among various species of macroorganisms, so the threshold is not precise. Regions with oxygen concentrations below about 10 $\mu\text{mol kg}^{-1}$ are termed suboxic. In suboxic regions, nitrate (if present) becomes involved in respiration (1). Anoxic regions have no dissolved oxygen. At present, the intermediate-depth low-oxygen layers, here called the oxygen-minimum zone (OMZ), are suboxic in the eastern tropical Pacific Ocean and the northern reaches of the tropical Indian Ocean and are hypoxic in the tropical Atlantic Ocean (Fig. 1).

Oceanic dissolved oxygen concentrations have varied widely in the geologic past. For instance,

paleoclimate records from the Cretaceous reveal profoundly altered biogeochemical cycles and dramatic consequences for ecosystems associated with reductions of ocean oxygen (4). The anoxic ocean at the end of the Permian (251 million years ago) is perhaps the most striking example, being associated with elevated atmospheric CO_2 and massive terrestrial and oceanic extinctions (5, 6).

Climate models predict an overall decline in oceanic dissolved oxygen concentration and a consequent expansion of the OMZ under global warming conditions (7), with the largest declines occurring in extratropical regions. In the tropical regions, the models predict either zonal mean oxygen increases at depths of about 200 to 1000 m in the Atlantic and Pacific Oceans (7) or moderate zonal mean oxygen decreases (8). Predicted oxygen changes in the thermocline waters result largely from solubility changes in the upstream source waters, whereas changes in the deeper waters result mainly from decreased interior advection and ongoing oxygen consumption by remineralization of sinking particulate organic matter (7).

The global ocean has warmed substantially over the past 50 years (9), and strong interannual-to-decadal variations of oxygen have been observed in the upper 100 m (10). Long-term oxygen changes have been observed and reported in the subpolar and subtropical regions (11, 12). For instance, in the subarctic Pacific at Ocean Station Papa (50°N, 145°W), declining oxygen concentrations have been reported from depths of 100 to 400 m between 1956 and 2006 (11). Ocean oxygen data from the most oxygen-poor tropical regions of the OMZ

¹Institut für Meereswissenschaften an der Universität Kiel (IFM-GEOMAR), Düsternbrooker Weg 20, 24105 Kiel, Germany.

²National Oceanic and Atmospheric Administration, Pacific Marine Environmental Laboratory, 7600 Sand Point Way NE, Seattle, WA 98115, USA. ³Scripps Institution of Oceanography, 9500 Gilman Drive, La Jolla, CA 92093, USA. ⁴Baltic Sea Research Institute Warnemünde, Post Office Box 301161, 18112 Rostock, Germany.

*To whom correspondence should be addressed. E-mail: lstramma@ifm-geomar.de